Scattering characteristics of cylindrical metamaterials

Ruey-Bing Hwang and Hsien-Tung Huang

Citation: AIP Advances **6**, 035107 (2016); doi: 10.1063/1.4943899
View online: http://dx.doi.org/10.1063/1.4943899
View Table of Contents: http://aip.scitation.org/toc/adv/6/3
Published by the American Institute of Physics

Scattering characteristics of cylindrical metamaterials

Ruey-Bing Hwang[a] and Hsien-Tung Huang
Electrical and Computer Engineering, National Chiao Tung University, Hsinchu, Taiwan

(Received 22 January 2016; accepted 29 February 2016; published online 8 March 2016)

This paper reports the scattering of electromagnetic plane wave by annular metamaterials composed of concentric regular dielectric layers of infinite length. Interestingly, in certain frequency ranges, their scattering properties are similar to those of a perfect electric conductor cylinder, except that the tangential electric field on their surfaces does not vanish. Moreover, the frequency bands of total reflection spectra can be rigorously predicted using Floquet–Bloch theorem.
[http://dx.doi.org/10.1063/1.4943899]

I. INTRODUCTION

The natural dielectric medium has its own specific refractive index. However, synthetic(artificial) dielectrics, which are usually periodic structures, provide flexibility in obtaining a desired effective permittivity or permeability from their physical structures instead of their chemical composition. Specifically, the dispersive and anisotropic characteristics of the effective refractive index of synthetic dielectrics can be rigorously analyzed using electromagnetic field theory.[2,3] Recently, metamaterials made of conventional materials such as metal and Epoxy were found to have extraordinary refractive indices, which are negative in a certain frequency band.[1]

Metamaterials were originally developed for creating an invisibility cloak, i.e., a covering for a metal object that makes it invisible to microwaves, millimeter waves, and light. Consequently, annular metamaterials are popularly designed for their symmetrical structure. Reported cases of such uses include, the echo-width calculation of a conducting cylinder coated with metamaterials,[4] the numerical analysis of radiation and scattering from concentric metamaterial cylinders excited by an electric line source,[5] the investigation of sub-wavelength resonances in metamaterial cylinders affected by the shape of the cylinder cross–section,[6] and a homogeneous isotropic invisibility cloak design based on geometrical optics.[7,8]

Planar metamaterials can be used to create mirrors for reflecting incident waves. Specifically, the tunable reflection phase can be employed to optimize the standing–wave profile to maximize light–matter interaction in planar devices.[9]

In this study, a cylindrical metamaterial made of conventional dielectrics is developed to mimic the scattering properties of a perfect electric conductor (PEC) cylinder in a certain frequency band. Because the periodicity of the unit cell is smaller than the wavelength of total reflection, the structure can be called metamaterial. Scattering fields, expressed using the superposition of cylindrical harmonics, are formulated analytically and calculated numerically. The underlying physics of wave processes involved are also discussed.

II. STRUCTURE CONFIGURATION

As shown in Fig. 1, the structure considered is composed of a cylinder filled with a uniform dielectric medium, with its radius and refractive index designated as r_c and n_c, respectively. The

[a]Corresponding author. Electronic mail: raybeam@mail.nctu.edu.tw

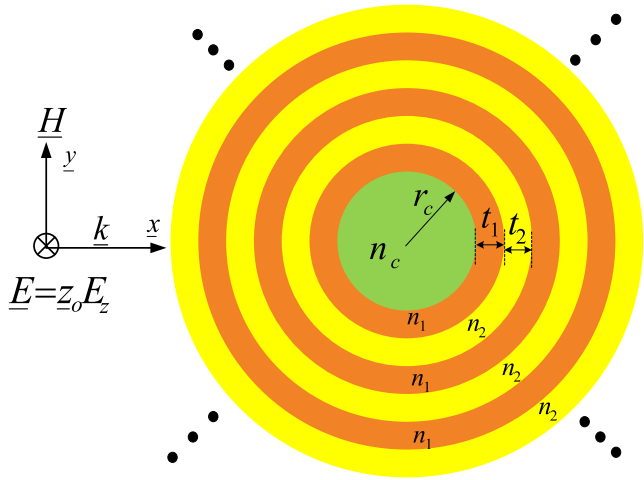

FIG. 1. Structure of the cylindrical metamaterial. Each unit cell along the radial direction is composed of two regular dielectric mediums, denoted as n_1 and n_2, with thicknesses t_1 and t_2, respectively. The core region has radius r_c and refractive index n_c.

region outside the core consists of multiple concentric dielectrics arranged in a one-dimensional periodic structure along the radial direction. The cylinder is assumed to be of infinite length (z-axis).

A plane electromagnetic wave is incident along the $+x$ axis. We assume that there is no field variation along the z-axis, i.e., $k_z = 0$. Electric and magnetic field problems can be regarded as 2D ones so that the E_z and H_z waves can be treated independently.

In the next section, mathematical procedures for performing the scattering analysis are summarized.

III. MATHEMATICAL ANALYSIS

Because the structure considered is a conical one, electric and magnetic fields can be expressed as superpositions of modal solutions in a cylindrical coordinate system, such as the Bessel, Neumann, and Hankel functions.[10–13] In this study, only the E_z-wave is elaborated because mathematical procedures for dealing with the H_z-wave are almost identical.

Tangential electric and magnetic field components, expressed in terms of the cylindrical coordinate system inside the m^{th} layer, can be written as

$$E_z^{(m)} = \sum_{n=0}^{n=\infty} \left[A_n^{(m)} J_n(k_m \rho) + B_n^{(m)} Y_n(k_m \rho) \right] \cos n\phi \tag{1}$$

$$H_\phi^{(m)} = -jY_m \sum_{n=0}^{n=\infty} \left[A_n^{(m)} J_n'(k_m \rho) + B_n^{(m)} Y_n'(k_m \rho) \right] \cos n\phi \tag{2}$$

where k_m and Y_m are the propagation constant and intrinsic admittance in the m^{th} layer, respectively, with electrical properties denoted as (μ_m, ε_m).

Because of electromagnetic boundary conditions, E_z and H_ϕ must be continuous at the interface between two dielectric layers denoted as layer m and layer $m + 1$, respectively. As a result, we obtain equations as follows:

$$A_n^{(m+1)} = t_{11} A_n^{(m)} + t_{12} B_n^{(m)} \tag{3}$$

$$B_n^{(m+1)} = t_{21} A_n^{(m)} + t_{22} B_n^{(m)} \tag{4}$$

where $A_n^{(j)}$ and $B_n^{(j)}$ are the Fourier amplitudes of the n_{th} order in the j_{th} layer. Parameters t_{11}, t_{12}, t_{21} and t_{22} are related to the radius (r_m), propagation constants (k_m and k_{m+1}), and admittances (Y_m and Y_{m+1}) in two adjacent layers.

The parameters t_{11}, t_{12}, t_{21}, and t_{22} are given as follows.

$$t_{11} = \tau_m \left[Y_n'(\zeta_{m+1}) J_n(\zeta_m) - x_m Y_n(\zeta_{m+1}) J_n'(\zeta_m) \right] \tag{5}$$

$$t_{12} = \tau_m \left[Y_n'(\zeta_{m+1}) Y_n(\zeta_m) - x_m Y_n(\zeta_{m+1}) Y_n'(\zeta_m) \right] \tag{6}$$

$$t_{21} = \tau_m \left[-J_n'(\zeta_{m+1}) J_n(\zeta_m) + x_m J_n(\zeta_{m+1}) J_n'(\zeta_m) \right] \tag{7}$$

$$t_{22} = \tau_m \left[-J_n'(\zeta_{m+1}) Y_n(\zeta_m) - x_m J_n(\zeta_{m+1}) Y_n'(\zeta_m) \right] \tag{8}$$

where parameters ζ_{m+1}, ζ_m, x_m and τ_m are defined as follows.

$$\zeta_{m+1} = k_{m+1} r_m \tag{9}$$

$$\zeta_m = k_m r_m \tag{10}$$

$$x_m = Y_m / Y_{m+1} \tag{11}$$

$$\tau_m = \pi k_{m+1} r_m / 2 \tag{12}$$

Here, Lommel's formula $J_v(x) Y_v'(x) - Y_v(x) J_v'(x) = \frac{2}{\pi x}$ was employed to calculate the parameters t_{11}, t_{12}, t_{21}, and t_{22}.

The tangential electric field outside the synthetic dielectric cylinder ($\rho >= b$) can be written as the superposition of the incident plane wave and scattering fields, both expressed in terms of cylindrical harmonics, which are written as

$$E_z^{(out)} = \sum_{n=0}^{n=\infty} \left[e_n j^{-n} J_n(k_o \rho) + C_n H_n^{(2)}(k_o \rho) \right] \cos n\phi \tag{13}$$

where $e_n = 1$ for $n = 0$ and $e_n = 2$ otherwise. The tangential electric field inside the core region can be written as

$$E_z^{(c)} = \sum_{n=0}^{n=\infty} A_n^{(0)} J_n(k_c \rho) \cos n\phi \tag{14}$$

By successively multiplying the transfer matrix defined at each interface with the elements given in (3) and (4) incorporated with the electromagnetic boundary conditions on the inner surface at $\rho = r_c$ and on the outermost surface at $\rho = b$, we can determine the Fourier amplitudes ($A_n{}^{(m)}$, $B_n{}^{(m)}$, and C_n) in each layer.

IV. NUMERICAL RESULTS

Consider the cylindrical metamaterial shown in Fig. 1. The core has radius $a = 500nm$ and the refractive index $n = 3.475$ (Silicon). There are ten periods in the radial direction. Each of the unit cells contains two dielectric mediums with refractive indices $n_1 = 1.45$ (Silica) and $n_2 = 3.475$, and thickness $t_1 = 100nm$ and $t_2 = 100nm$, respectively. The radius of the metamaterial cylinder is $b = 2500nm$.

To observe the scattering characteristics of the metamaterial cylinder, photons with energies of $1.2eV$ are incident on the structure and the normalized scattering echo width versus the observation angle ϕ is calculated, as shown in Fig. 2. Here, two counterparts, cylinders made of PEC and Au, which share the same dimensions as the metamaterial cylinder, are also subjected to the scattering analysis. Interestingly, the three cases exhibit almost the same scattering properties from $\phi = 0°$ to $\phi = 360°$. However, a discrepancy is observed in the forward scattering region around $\phi = 180°$, as shown in the inset of Fig. 2. The echo widths of the PEC and the metamaterial are slightly larger than that of the gold cylinder. That is due to loss by Au absorption. Figure 3 shows the dielectric function, which is based on the Lorentz-Drude model,[14] of gold, with a plasma frequency of $8.5eV$ and a damping frequency of $0.048eV$. The absorption is caused by the nonzero imaginary part ε_i.

The photon energy is changed to $2.0eV$ and the bi-static echo width is recalculated. In Fig. 4, we observe a totally different scattering scenario: the incident plane wave is scattered drastically by the metamaterial. By contrast,the echo-width patterns of the gold and PEC cylinders stay the same, as shown in Fig. 2. From these two distinct results, we understand that the scattering characteristics

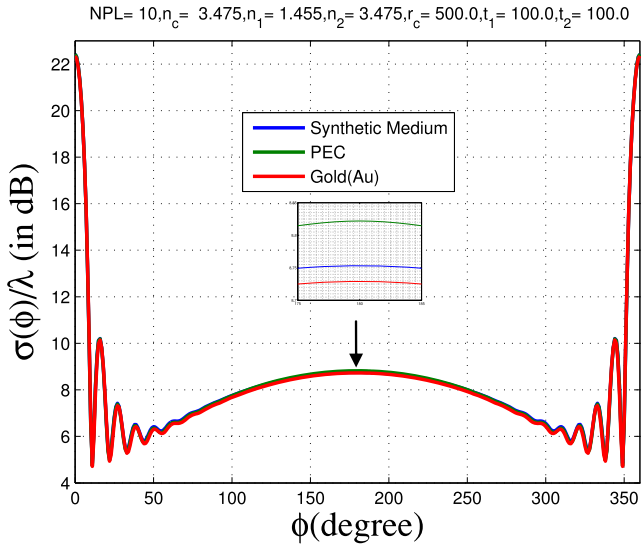

FIG. 2. Variation of the normalized echo width against ϕ at $1.2eV$ for the three materials, including a perfect electrical conductor, Au and the metamaterial. They share the same diameter of $2500nm$.

of the metamaterial are frequency dependent. Therefore, the scattering spectra should be studied in detail in order to reveal the underlying physics of this class of metamaterials.

Figure 5 shows the total echo width $\sigma(\phi)$ normalized to the operation wavelength, where the total normalized echo width is defined as the integration of $\sigma(\phi)/\lambda$ over the azimuthal angle (ϕ) from 0 to 2π. The total echo widths of the two counterparts are also calculated. Notably, the relative dielectric constant of Au is a complex number with negative ε_r in the frequency range of operation. Therefore, the incident wave is reflected back into the air due to the electromagnetic fields attenuation inside the gold.

Returning to Fig. 5, the scattering properties of the metamaterial are similar to those of the PEC and Au cylinders when the incident photons have energies in the regions $[1.2eV, 1.5eV]$ and $[2.2eV, 3eV]$. The echo width of the Au cylinder is slightly smaller than those of the PEC and the metamaterial owing to the obvious dielectric loss as mentioned previously. Outside these ranges the echo width, generally, fluctuates strongly and deviates from those of the PEC and gold cylinders.

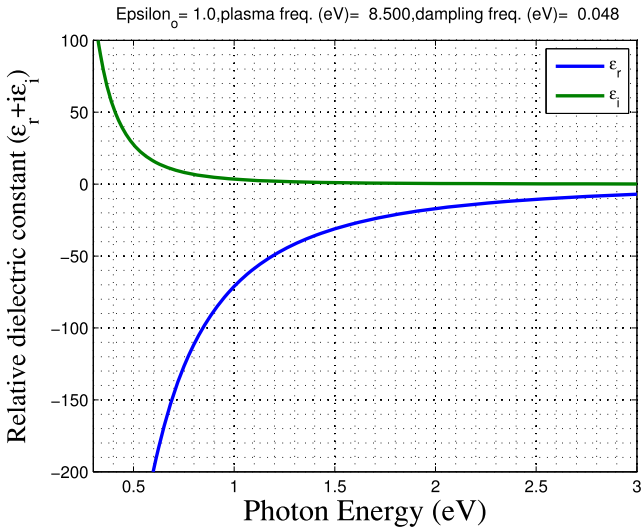

FIG. 3. The dielectric function of Au including the real and imaginary parts of the relative dielectric constant.

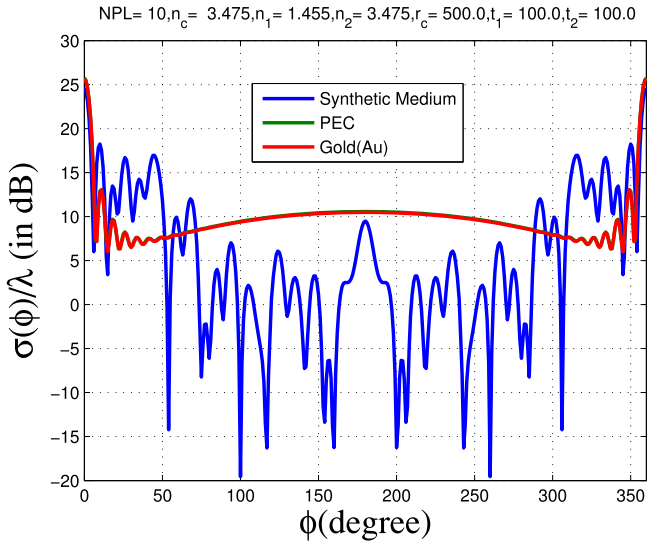

FIG. 4. Variation of the normalized echo width versus ϕ for the three materials (PEC, Au and the metamaterial).

This figure indicates that the metamaterial cylinder can mimic the scattering characteristics of a metallic one in certain frequency bands.

The contour map of the constant electric field is also plotted, in order to demonstrate the scattering behavior of the metamaterial cylinder. Figure 6 shows the real part of $E_z(x, y)$ over the 2D plane at a photon energy of $2eV(620nm)$. Due to the non uniform refractive index, the scattering pattern is very different from that of a uniform dielectric cylinder. For example, although it is not shown here, the corresponding dielectric cylinder with $n = 1.455$, at this frequency, will focus the incident wave onto a point on the opposite side of the cylinder and re-radiate it, as from a point source, into free space.

A second example is the case with photons of energy $1.2eV$. As we know from Fig. 5, its total echo width is almost equal to that of PEC and gold at this frequency. It appears that the electric field penetrating the metamaterial exponentially decays to zero. A shadow region behind the cylinder can be observed. Moreover, the z-component of the electric-field strength ($|E_z(x, y = 0)|$) along the x-axis is plotted, and it is found that E_z does not vanish on the surface of the cylinder (the left-hand

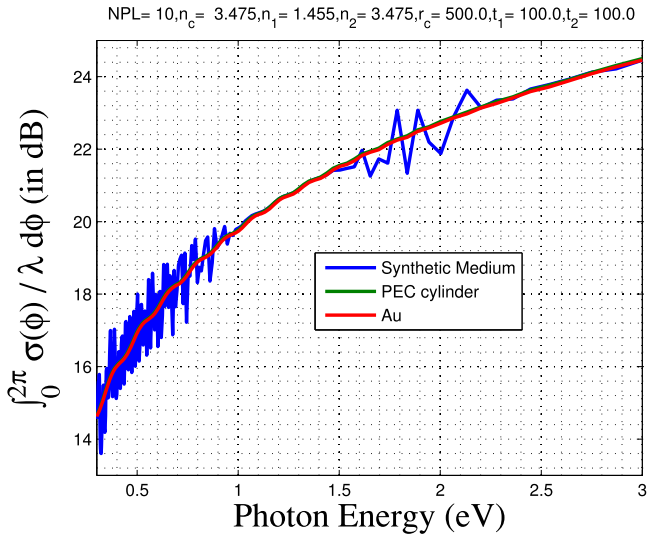

FIG. 5. Variation of the normalized total echo width against the photon Energy (in eV) for the three materials.

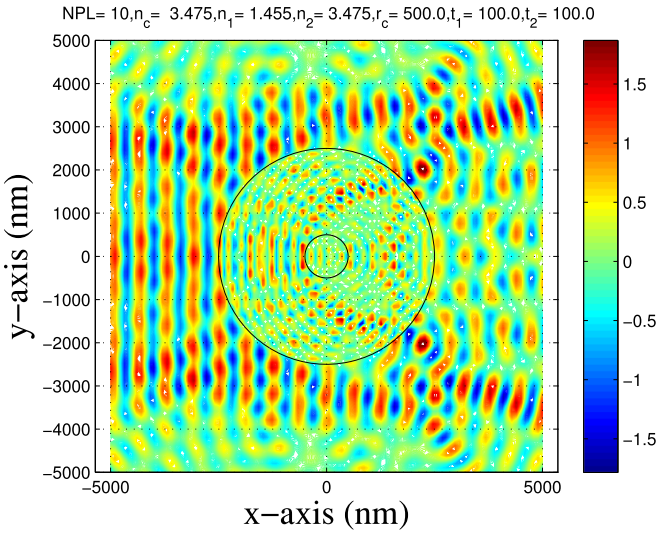

FIG. 6. The distribution of the real part z-component electric field along the 2D plane. Photons of energy $2.0eV$ are incident on the structure.

side interface between the cylinder and air is highlighted by the red line). Unlike when a plane wave impinges upon a metal surface, the reflected wave is not at all out-of-phase with the incident one. Thus, the total E_z on the interface is not zero, as shown in Fig. 7(b). It may be conjectured that the input impedance (from a transmission-line analogy) of the periodic concentric dielectric layers is a purely imaginary reactive one, which may be inductive or capacitive. Consequently, the incident power is reflected back into the air. Additionally, the exponential decay along the x-axis means that the electromagnetic wave inside the metamaterial has a non-zero attenuation constant.

Returning to Eqs. (1) and (2), if the ρ-components in these two equations are denoted as $v_n(\rho)$ and $i_n(\rho)$, the input and output relation of the voltage and current waves between the two interfaces at $\rho = \rho_o$ and $\rho = \rho_o + t_m$ can be written as follows, where t_m is the thickness of dielectric layer m, and ρ_o is the radius of the inner cylinder.

$$\begin{bmatrix} V_n^{(m)}(\rho_o + t_m) \\ I_n^{(m)}(\rho_o + t_m) \end{bmatrix} = \mathbf{T}^{(m)} \begin{bmatrix} V_n^{(m)}(\rho_o) \\ I_n^{(m)}(\rho_o) \end{bmatrix} \tag{15}$$

$$\mathbf{T}^{(m)} = \frac{\pi k_m \rho_0}{2} \begin{pmatrix} Y_n'(k_m\rho_0)J_n(k_m\rho) - J_n'(k_m\rho_0)Y_n(k_m\rho) & Z_m\left[J_n(k_m\rho_0)Y_n(k_m\rho) - Y_n(k_m\rho_0)J_n(k_m\rho)\right] \\ Y_m\left[Y_n'(k_m\rho_0)J_n'(k_m\rho) - J_n'(k_m\rho_0)Y_n'(k_m\rho)\right] & J_n(k_m\rho_0)Y_n'(k_m\rho) - Y_n(k_m\rho_0)J_n'(k_m\rho) \end{pmatrix} \tag{16}$$

where the parameter $\mathbf{T^{(m)}}$ is the transfer- (or ABCD-) matrix of dielectric layer m. It is a 2-by-2 matrix with each element related to the parameters m, n, ρ_o, t_m, and k_m. Therefore, the transfer matrix of the unit cell consisting of two dielectric layers can be simply expressed as the product of the two individual transfer matrices, written as

$$\begin{bmatrix} V_n^{(2)}(\rho_o + t) \\ I_n^{(2)}(\rho_o + t) \end{bmatrix} = \mathbf{T}^{(2)} \cdot \mathbf{T}^{(1)} \begin{bmatrix} V_n^{(1)}(\rho_o) \\ I_n^{(1)}(\rho_o) \end{bmatrix} \tag{17}$$

where $t(= t_1 + t_2)$ is the period of the unit cell along the radial direction.

According to the periodic boundary condition in a cylindrical coordinate system,[15] the input-output relation of the voltage and current waves through a period along the ρ-direction satisfies the following equation:

$$\sqrt{\rho_o + t} \begin{bmatrix} V_n^{(2)}(\rho_o + t) \\ I_n^{(2)}(\rho_o + t) \end{bmatrix} = \lambda \sqrt{\rho_o} \begin{bmatrix} V_n^{(1)}(\rho_o) \\ I_n^{(1)}(\rho_o) \end{bmatrix} \tag{18}$$

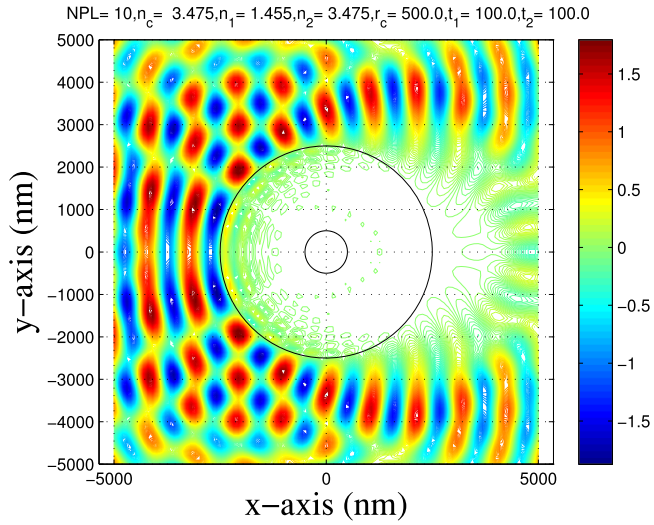

(a)

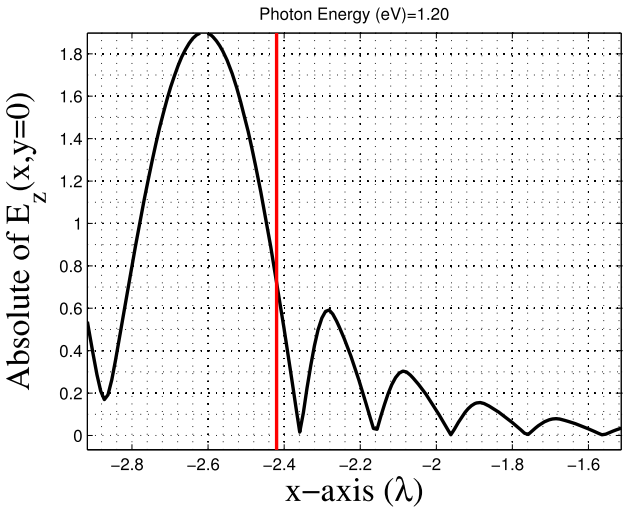

(b)

FIG. 7. The distribution of the z-axis electric field component along the 2D plane. A plane wave with photon energies of $1.2eV$ is incident on the structure. (a) The real part of $E_z(x, y)$, and (b) the strength of $E_z(x, y = 0)$.

where λ is the eigenvalue equal to $\exp(\pm ik_\rho t)$, and k_ρ is the effective propagation constant along the ρ-direction. By substituting Eq. (17) into Eq. (18), we create the following eigenvalue problem.

$$\mathbf{T}^{(2)} \cdot \mathbf{T}^{(1)} \begin{bmatrix} V_n^{(1)}(\rho_o) \\ I_n^{(1)}(\rho_o) \end{bmatrix} = \lambda \sqrt{\frac{\rho_o}{\rho_o + t}} \begin{bmatrix} V_n^{(1)}(\rho_o) \\ I_n^{(1)}(\rho_o) \end{bmatrix} \tag{19}$$

We can determine the two eigenvalues and the effective propagation constant including the phase (β_ρ) and attenuation (α_ρ) constants along the ρ-axis.

Figure 8 shows the dispersion relation of the wave propagation along the radial direction. The effective phase (β_ρ)- and the attenuation (α_ρ)-constants, which are individually shown on the left-hand and right-hand sides, respectively, have been normalized in order to present them in terms of the traditionally used Brillouin diagram.[3] The regions from $1.0eV$ to $1.5eV$ and from $2.2eV$ to $2.9eV$ have non-zero attenuation constants. Inside these two regions, the wave decays exponentially along the propagation direction. They are so-called stop-band (band-gap) regions. Regions outside the stop bands are called pass-band ones, where the waves can propagate.

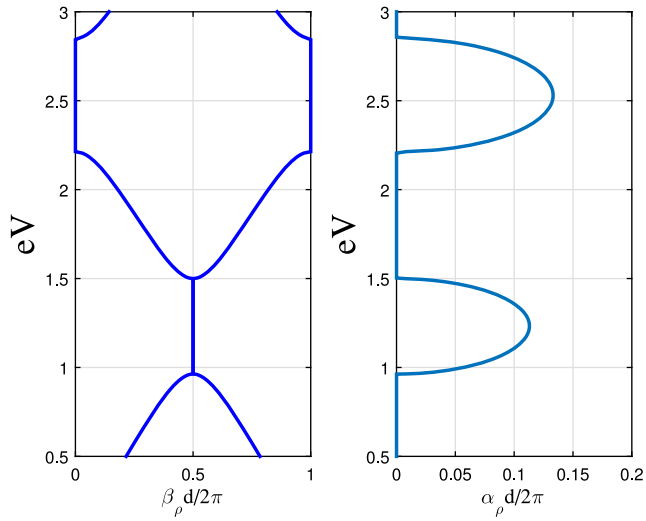

FIG. 8. Brillouin diagram of the cylindrical periodic structure with a periodicity along the radial direction. The two dielectric mediums have refractive indices $n_1 = 1.455$ and $n_2 = 3.475$, their thickness are both $100nm$, and the 0-th order cylindrical harmonic index is considered.

V. CONCLUSION

An annular metamaterial was developed using alternating silicon and silicon dioxide layers along the radial direction. Due to the periodic boundary conditions, the wave propagation along the radial direction was found to exhibit stop- and pass-bands, enabling total reflection in band-gap regions. Significantly, the tangential component of the electric field was observed not to vanish on the metamaterial surface during total reflection. This structure can mimic a PEC cylinder, but at the same time, its non-zero tangential electric field near its surface has some additional applications in optoelectronic device design.

ACKNOWLEDGEMENTS

The corresponding author (Prof. Ruey-Bing Hwang) would thank Ministry of Science and Technology, Taiwan for their support in the project under the contract: MOST 104-2221-E-009 -111 -.

[1] R. A. Shelby, D. R. Smith, S. C. Nemat-Nasser, and S. Schultz, "Microwave transmission through a two-dimensional, isotropic, left-handed metamaterial," Applied Physics Letter **78**(4), 489–491 (2001).
[2] R. E. Collin, *Field Theory of Guided Waves*, 2nd ed. (Wiley-IEEE Press, 1990).
[3] Ruey-Bing (Raybeam) Hwang, *Periodic Structures: Mode-Matching and Applications in Electromagnetic Engineering* (Wiely-IEEE Press, 2013).
[4] C. Li and Z. Shen, "Electromagnetic scattering by a conducting cylinder coated with metamaterials," Progress In Electromagnetics Research **42**, 91–105 (2003).
[5] S. Arslanagi?, R. W. Ziolkowski, and O. Breinbjerg, "Analytical and numerical investigation of the radiation and scattering from concentric metamaterial cylinders excited by an electric line source," Radio Sci. **42**(6), RS6S15 (2007).
[6] S. Arslanagi? and O. Breinbjerg, "A numerical investigation of sub-wavelength resonances in polygonal metamaterial cylinders," Optics Express **17**(18), 16059–16072 (2009).
[7] J. Sun, J. Zhou, and L. Kang, "Homogenous isotropic invisible cloak based on geometrical optics," Optics Express **16**(22), 17768–17773 (2008).
[8] G.P. Zouros, J.A. Roumeliotis, and G.T. Stathis, "Electromagnetic scattering by an infinite cylinder of material or metamaterial coating eccentrically a dielectric cylinde," J Opt Soc Am A Opt Image Sci Vis. **28**(6), 1076–85 (2011).
[9] M. Esfandyarpour, E. C. Garnett, Y. Cui, M. D. McGehee, and M. L. Brongersma, "Metamaterial mirrors in optoelectronic devices," Nature Nanotechnology **9**, 542–547 (2014).
[10] C. C. H. Tang, "Backscattering from dielectrically coated infinite cylindrical obstacles," J. Appl. Phys. **28**, 628–633 (1957).
[11] H. Massoudi, N. J. Damaskos, and P. L. E. Uslenghi, "Scattering by a composite and anisotropic circular cylindrical structures," Electromagnetics **8**, 71–83 (1988).

[12] A. Z. Elsherbeni and A. A. Kishk, "Modeling of cylindrical objects by circular dielectric and conducting cylinders," IEEE Trans. Antennas Propagation **40**(1), 96–99 (1992).
[13] A. A. Kishk, R. P. Parrikar, and A. Z. Elsherbeni, "Electromagnetic scattering from an eccentric multilayered circular cylinder," IEEE Trans. on Antennas and Propagation **40**, 295–303 (1992).
[14] R. L. Olmon, B. Slovick, T. W. Johnson, D. Shelton, S.-H. Oh, G. D. Boreman, and M. B. Raschke, "Optical dielectric function of gold," Phys. Rev. B **86**, 235147 (2012).
[15] A. Kitagawa and J.-i. Sakai, "Bloch theorem in cylindrical coordinates and its application to a Bragg fiber," Phys. Rev. A **80**, 033802 (2009).